Chemical Engineering Journal 111 (2005) 213–223

Chemical Engineering Journal

www.elsevier.com/locate/cej

The role of wave propagation in hydrocyclone operations II: Wave propagation in the air–water interface of a conical hydrocyclone

E. Ovalle, F. Concha *

Department of Metallurgical Engineering, University of Concepción, Concepción, Chile

Abstract

The air-core plays an important role in the operation of a conical hydrocyclone. In the apex, the air-core increases in diameter with the possibility of reaching a size close to the apex diameter. In this case, roping may be induced. There is a range of values for the apex to vortex ratio where roping is possible. Using some simple physical models, this work shows that perturbations propagating through the air-core interface are amplified in the direction of the apex and may be responsible for the fluctuations of the underflow that are characteristic of roping.
© 2005 Published by Elsevier B.V.

Keywords: Hydrocyclone; Wave motion

1. Introduction

In previous work [10], we discussed the flow pattern in a conical hydrocyclone and obtained a numerical solution of the Navier–Stokes equation by the finite element method (FEM). In the present work, we focus on the existence and propagation of wave motion inside a conical hydrocyclone.

From a practical point of view, the principal interests are the efficiency of the classification process and in the operational stability of the hydrocyclone performance. The efficiency of classification is characterized by the sharpness of the separation, which can be visualized by the shape of the classification curve. In a numerical hydrocyclone model, the classification curve may be obtained by introducing particles in the flow field and following the trajectories. These trajectories are sensitive to the perturbations introduced by the instabilities of flow, and the presence of turbulence. In the presence of these phenomena, the classification curve is less sharp.

One feature that complicates the study of the flow in a conical hydrocyclone, is the presence of an air-core [1,4,6]. Electrical resistance tomography studies have shown that the air-core is not static [12], and some experimental observations show that the instabilities of the air-core could produce a degradation in the classification quality [9]. We think that perturbations induced by wave propagation in the flow may also influence the efficiency.

In this paper, the problem of generation and propagation of waves in a hydrocyclone is addressed. Through a hydraulic analogy, the study starts modelling the flow inside a conical hydrocyclone, where the centrifugal force is replaced by a gravitational force. In this context, it is possible to study some particular features of the flow such as the form adopted by the free surface, the propagation of superficial waves through the air–water interface, and the effect of the waves on the operation of a conical hydrocyclone. Next, we propose a possible mechanism for the generation of wave motions in a region adjacent to the air-core of a hydrocyclone.

2. Form of the free surface

The form of the free surface observed in a laboratory hydrocyclone is similar to that shown in Fig. 7. The surface is horizontal and flat (cylindrical in the actual case) and deformed in the outlet regions. As we will show, these deformations are evidence for the existence of wave-like motions in the region near to the air-core.

Consider, for example, the flow in a channel with a constant depth H [11] (see Fig. 1), where the flow has an upstream constant velocity U. If, in a certain region, a ramp is present

* Corresponding author.

1385-8947/$ – see front matter © 2005 Published by Elsevier B.V.
doi:10.1016/j.cej.2005.02.010

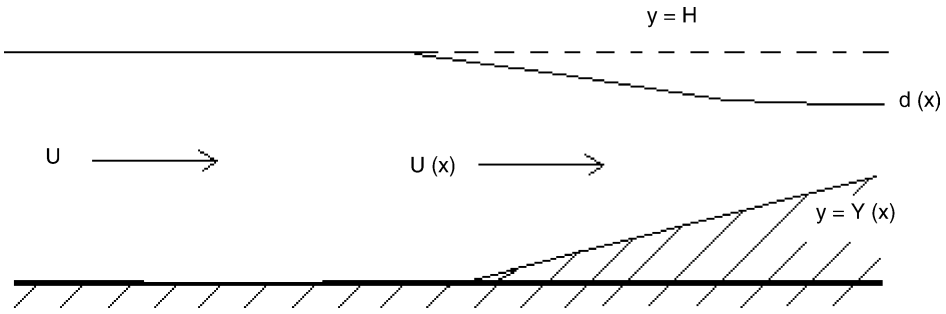

Fig. 1. Free-surface deformation in a channel.

in the form $y = Y(x)$, the height of the free surface will change from $y = H$ to $y(x) = H - d(x)$. The conservation of mass demands that:

$$UH = u(x)[H - d(x) - Y(x)] \tag{1}$$

On the other hand, momentum is conserved in the flow and may be expressed by the Bernoulli equation over a free surface streamline:[1]

$$\frac{1}{2}U^2 + gH + \frac{p}{\rho} = \frac{1}{2}u^2 + g(H - d) + \frac{p}{\rho} \tag{2}$$

Eliminating $u(x)$ from the above equations results in:

$$\frac{U^2H^2}{(H - d - Y)^2} = U^2 + 2gd \tag{3}$$

Since $d \ll H$, the LHS of Eq. (3) can be expanded in a rapidly convergent series. Truncating this series yields:

$$d(x) = \frac{Y(x)}{F^{-2} - 1} \tag{4}$$

where F is the Froude number defined by:

$$F = \frac{U}{\sqrt{gH}} \tag{5}$$

The flow is *subcritical* when $F < 1$ and *supercritical* when $F > 1$. In the first case, $d(x)$ has the same sign as $Y(x)$ and the free surface decreases its level downstream. The inverse occurs when $F > 1$. This change of regime, associated with the variation of the Froude number, determines how a perturbation is propagated through the flow. As is known in the shallow-water theory, the wave velocity of propagation c is proportional to $\sqrt{gH}$. Therefore, the Froude number, written as $F = \frac{U}{c}$, has a physical meaning similar to the Mach number in compressible flows. If the flow is supercritical, the velocity of the fluid is greater than the transmission of information about a change in the floor level; thus, the perturbation upstream has no effect on the flow downstream. In the opposite case, the information may advance faster than the flow, and the perturbations originated at the floor are reflected upstream, which are favorable conditions for the formation of waves in the flow.

In a conical hydrocyclone, the flow has a tangential component that is the same order of magnitude as the axial component except at the outlet region where the axial component is increased at the expense of the tangential component. Therefore, based on the observations of the free surface in the adjacent outlet regions, we assume that, *inside the hydrocyclone, the flow is in a subcritical state and, as a consequence, this condition is favorable for the existence of undulatory motions in the fluid*.

3. The hydraulic model

The work of Escudier et al. [8], who used a hydraulic analogy to study the change between subcritical and supercritical regimes of a swirly flow, inspired us to study the propagation of waves in the air-core of a hydrocyclone in a similar manner. The hydraulic model of the hydrocyclone consists of a launder with a ramp as shown in Fig. 2. The water enters through the bottom at the left side and overflows at the left and right of the upper part of the model.

The model is a bi-dimensional, Cartesian representation of a conical hydrocyclone geometry, as is shown in Fig. 2. In this representation, the centrifugal force is replaced by gravitational force, $-\rho\mathbf{g}$, in the vertical direction. The flow is modelled as inviscid and irrotational and the velocity is expressed in terms of a potential velocity $\mathbf{v} = \nabla\phi$. This approach has the following advantages: the boundary conditions can be chosen with a clear physical sense, in contrast with other formulations (for example, the stream-vorticity scheme). The second reason for this formulation is because the treatment of the undulatory phenomena is more direct.

In the model, the flow obeys: the continuity equation $\nabla^2\phi = 0$ and Bernoulli's equation of motion:

$$B(t) = \frac{\partial\phi}{\partial t} + \frac{1}{2}|\nabla\phi|^2 + gy + \frac{p}{\rho} \tag{6}$$

where p is the pressure field, $B(t)$ an arbitrary function of time, ρ the constant liquid density and g is the gravitational acceleration. Since the potential ϕ, is only unique up to a constant,

[1] In the hydrocyclone case, a centrifugal force $m\frac{v_r^2}{r}$ must be considered in Eq. (2).

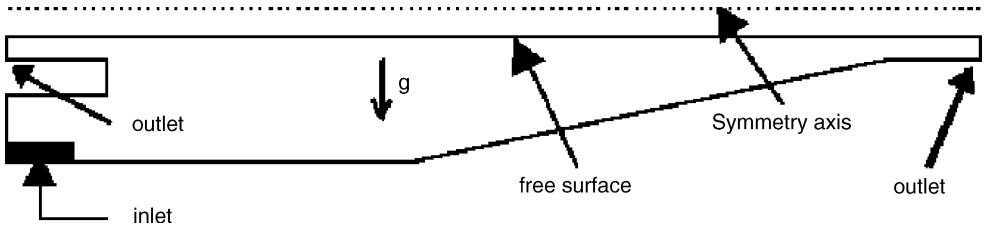

Fig. 2. Hydraulic analogy of a conical hydrocyclone.

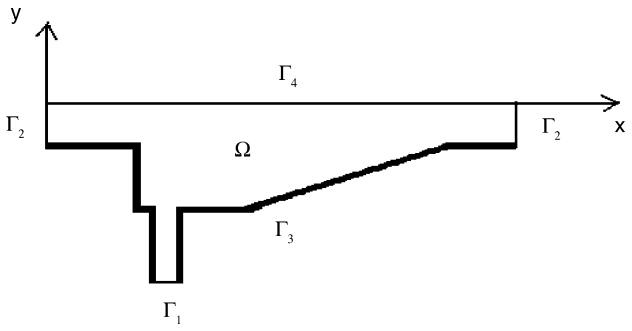

Fig. 3. Simplified hydraulic model of a hydrocyclone.

we can take $B(t) \equiv 0$. The last equation can be considered a definition for the pressure field in the stationary case. It contains two terms: a hydrostatic force, $-gy$, and the dynamical component given by the velocity field $\frac{1}{2}|\nabla\phi|^2$.

The simplified hydraulic model is shown in Fig. 3. The domain of the problem is denoted by Ω and the boundaries by $\Gamma = \{\Gamma_1 \cup \Gamma_2 \cup \Gamma_3 \cup \Gamma_4\}$, where Γ_1 is an inlet region, Γ_2 outlet regions, Γ_3 the walls and Γ_4 is the free surface. In the model, we use Cartesian coordinates (x, y) and the two-dimensional velocity will be given by $\mathbf{v} \equiv (u, v)$.

The problem can now be expressed in the following form: over Ω, the Laplace equation $\nabla^2\phi = 0$ needs to be satisfied. At Γ_1, the flow is fixed through the inlet velocity $v_{\text{in}} = \partial\phi/\partial n$, the normal component of ϕ. At the outlet regions, we fixed the values of ϕ to arbitrary constant values C_1 and C_2.[2] Since the flow has no viscosity, we set the normal component of the velocity field equal to zero at the walls. Finally, we impose a particular differential equation at the free surface Γ_4, as will be shown.

At this free surface, it is necessary to impose two complementary conditions. The *kinematical condition* expresses the fact that the position of the free surface is coincident with the border of the fluid, every time and everywhere. Experimental observations have shown that if a fluid particle is located over the free surface at a given time, it remains there forever. If the interface position is described by a function $y = \eta(x, t)$, where y is the position of a particle of fluid and η represents the position of the free surface, then the restriction is expressed mathematically by $f(x, y, t) = y - \eta(x, t) = 0$. This condition can be rewritten in terms of a material derivative of f as:

$$\frac{Df}{Dt} \equiv \frac{\partial f}{\partial t} + \nabla f \cdot \mathbf{v} = 0 \tag{7}$$

where u and v are the horizontal and vertical components of $\mathbf{v}$. From the definition of f, the last expression adopts the form:

$$\frac{\partial \eta}{\partial t} + \frac{\partial \phi}{\partial x}\frac{\partial \eta}{\partial x} - \frac{\partial \phi}{\partial y} = 0 \tag{8}$$

The second condition is *dynamical* and considers the pressure distribution over the free surface. If the properties of the water–air interface are neglected,[3] the pressure can be considered constant over the free surface, and its value fixed to an arbitrary constant, ϕ_0, in the Bernoulli Eq. (6). If $\eta(x, t)$ denotes the height of the free surface with respect to an arbitrary level of reference $y = 0$, Bernoulli's equation can be rewritten for the free surface in terms of the deformation, η as:

$$\frac{\partial \phi}{\partial t} + \frac{1}{2}|\nabla\phi|^2 + g\eta = 0 \tag{9}$$

where we have chosen $p_0 = 0$ for convenience. The problem can be set formally as follows: consider a domain Ω having a free surface at the boundary Γ_4. Then, in Ω, the velocity potential satisfies the Laplace equation $\nabla^2\phi = 0$ and, over Γ, the two Eqs. (2) and (8). In the literature, a number of numerical methods exist to solve these equations. Nevertheless, the problem can be solved using a simple iterative method. Since the pressure is the same at all points on the free surface, we can choose a reference point P_1 there, and on the free surface, use the Bernoulli Eq. (6) to calculate the deformation on both sides of P_1. Then, for a neighboring point P_2, the new deformation, η_2, is:

$$\eta_2 = \eta_1 + \frac{1}{2g}(\mathbf{v}_1^2 - \mathbf{v}_2^2) \tag{10}$$

With this simple procedure, we can calculate the *form* of the free surface but not its absolute *position*. To obtain the position, we need to minimize a functional constructed in terms of the total mechanical energy of the flow, simply choosing the case when the total pressure drop is an extremum. The

[2] The case, $C_1 \neq C_2$, can be considered as an external gradient of ϕ imposed on the main flow in the horizontal direction. In the real case, when the hydrocyclone operate in a vertical position, these constants can be used to represent the contribution of the gravity field in the vertical direction.

[3] We will not consider the effect of superficial stress, i.e., due to chemical additives to the fluid.

justification for using the method is that, in nature, physical processes tend to utilize a minimum amount of energy.

We developed a FEM code in MATLAB to solve the equations of the hydraulic model and the commercial code (FLUENT) to obtain the form of the free surface in a hydrocyclone. In these simulations, we used cylindrical coordinates and the problem was defined as axisymmetric. To obtain good results, it was necessary to use a simple RNG model in the first steps and a second-order differential turbulence model afterwards. A great advantage in using FLUENT in Unix was the possibility to use a mesh generator (*preFC*) in an iterative or batch mode that can be set through a series of commands written in a text (Ascii) file. In this way, the deformation of the free surface was calculated, correcting the form to obtain an uniform pressure distribution. Example results doing the previous calculation steps are shown in Fig. 4.

Some authors have suggested that the form of the air-core can be determined by some mechanical characteristics of the free surface through a dynamical restriction [3,7]. They say that if T_{rr} is the normal (radial) stress inside a fluid, the radius of the air-core, r_{ac}, can be calculated by using the Young–Laplace equation:

$$[T_{rr}]_{r=r_{ac}} = -\frac{\sigma}{R} \tag{11}$$

where $[T_{rr}]_{r=R} = T_{rr}|_{\text{water}} - T_{rr}|_{\text{air}}$ and σ is the liquid–air interface tension. The radial stresses in a viscous liquid with viscosity μ, can be estimated using a first-order expansion of r in the form:

$$T_{rr} = -p + 2\mu\frac{\partial v_r}{\partial r} \tag{12}$$

If α represents the radial gradient of the radial velocity v_r, Eq. (12) can be written as $T_{rr} = -p + 2\,\mu\alpha$. From (11) and (12), the diameter of the air-core is:

$$d_a = \frac{2\sigma}{\Delta p - 2\mu\alpha} \tag{13}$$

This theory can be applied in an inverse sense. The calculations show that using a simple hydraulic model or a commercial code to solve the full Navier–Stokes equations, it is possible obtain the right form and position of the free surface, without any use of additional physicochemical properties of the interface. The Young–Laplace equation can be used for calculate the pressure jump in the interface, although technically is difficult by the evaluation of the $\alpha = \partial v_r/\partial r$ term. However, this is technically difficult and the results are highly variable. It is our opinion that despite the theoretical attractiveness and sophistication of the theory, its application in the inverse sense (the calculation of the diameter from the known pressure) is not necessarily valid. It can be concluded that the form of the free surface is determined mainly by global properties of the geometry and flow and only in a minor extent by local properties of the surface, such as the surface tension.

3.1. Waves

The second problem to consider is the propagation characteristics of waves at the free surface. As was mentioned before, the form of the free surface in the hydrocyclone supports the existence of wave-like motions in its interior. The first task is to incorporate an expression for the normal component of the velocity at the free surface in the kinematical boundary condition.

The unit normal **n** of the free surface $f(x, y, t) = 0$ is given by the normalized gradient of f:

$$\mathbf{n} = \frac{\nabla\phi}{|\nabla\phi|} = \frac{\frac{\partial f}{\partial x}\mathbf{i} + \frac{\partial f}{\partial y}\mathbf{j}}{\sqrt{\left(\frac{\partial f}{\partial x}\right)^2 + \left(\frac{\partial f}{\partial y}\right)^2}} \tag{14}$$

Now, it is possible to calculate the normal component of the velocity field in the direction of **n**:

$$\frac{\partial\phi}{\partial n} = \mathbf{n}\cdot\nabla\phi = \frac{u\frac{\partial f}{\partial x} + v\frac{\partial f}{\partial y}}{\sqrt{\left(\frac{\partial f}{\partial x}\right)^2 + \left(\frac{\partial f}{\partial y}\right)^2}} = \frac{-\frac{\partial f}{\partial t}}{\sqrt{\left(\frac{\partial f}{\partial x}\right)^2 + \left(\frac{\partial f}{\partial y}\right)^2}} \tag{15}$$

or in terms of y and η:

$$\frac{\partial\phi}{\partial n} = \frac{\frac{\partial\eta}{\partial t}}{\sqrt{1 + \left(\frac{\partial\eta}{\partial x}\right)^2}} = \frac{\frac{\partial\eta}{\partial t}}{\sqrt{1 + \tan^2(\theta)}} = \frac{\partial\eta}{\partial t}\cos(\theta) \tag{16}$$

where we have replaced $\partial n/\partial x$ by $\tan(\theta)$ which represents the slope of the surface element respect to the horizontal direction. Another form to obtain (16) is as follows: define **s** and **n** as the unit vectors oriented in the tangential and normal direction relative to the free surface. In terms of θ, we have $\mathbf{s} = \cos(\theta)\mathbf{i} + \sin(\theta)\mathbf{j}$ and $\mathbf{n} = -\sin(\theta)\mathbf{i} + \cos(\theta)\mathbf{j}$. Then,

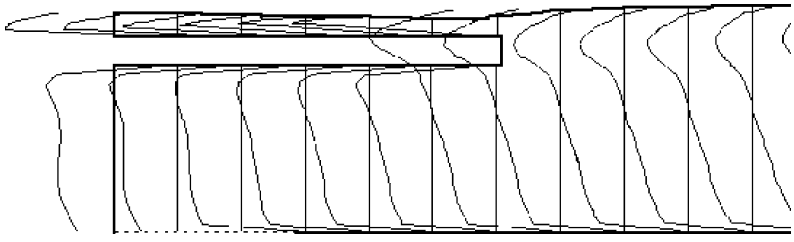

Fig. 4. Variations in free surface height.

$(\partial\phi/\partial n) = \mathbf{n}\cdot\nabla\phi = -\sin(\theta)(\partial\phi/\partial x) + \cos(\theta)(\partial\phi/\partial y)$. By (8), $(\partial\eta/\partial t) + (\partial\phi/\partial x)\tan(\theta) - (\partial\phi/\partial y) = 0$. From the two last expressions, we have $(\partial\phi/\partial n) = (\partial\eta/\partial t)\cos(\theta)$.

Now, we can linearize the kinematical and dynamical conditions if we neglect the terms proportional to $|\nabla\phi|^2$ and $\frac{\partial\psi}{\partial x}\frac{\partial\eta}{\partial x}$. Then, Eqs. (8) and (9), are replaced by:

$$\frac{\partial\phi}{\partial t} + g\eta = 0 \tag{17}$$

$$\frac{\partial\eta}{\partial t} - \frac{\partial\phi}{\partial y} = 0 \tag{18}$$

Now, we can combine the above equations to obtain a hyperbolic differential equation having the form of a wave equation:

$$\frac{\partial^2\phi}{\partial t^2} + g\frac{\partial\phi}{\partial n}\sqrt{1+\tan^2(\theta)} = 0 \tag{19}$$

If θ is small, then $\tan(\theta)\approx 0$ and $\partial\phi/\partial n \approx \partial\phi/\partial y$. Furthermore, if we impose a periodic perturbation $\phi(x, y, t) = \phi_0(x, y)\,e^{i\omega t}$ over the free surface, we obtain the following equation for ϕ:

$$\frac{\partial\phi}{\partial n} = \frac{\omega^2}{g}\phi \tag{20}$$

Eq. (20) is a Robin boundary condition. When it is applied over the free surface Γ_4, the dynamics of the free surface are transmitted to the interior Ω, where the Laplace equation $\nabla^2\phi = 0$ is satisfied.

For a better illustration, consider the case of stationary waves in the form $\phi(x, y, t) = f(x)g(y)\,e^{i\omega t}$. For this selection, the Laplace equation imposes:

$$\frac{f''}{f} + \frac{g''}{g} = 0 \tag{21}$$

at each point in Ω.

This equation is satisfied only if $f''/f = -g''/g =$ constant. If the constant is negative, say $-k^2$, then the differential equation for $f(x)$ has the form of an harmonic oscillator, where k represents the spatial frequency $k = 2\pi/\lambda$ for a given wavelength λ. Then, $f(x)$ can be expressed in terms of the sinusoidal function $A\cdot\sin(kx+\alpha)$, with α being a phase constant. In a similar form, $g(y)$ can be expressed in terms of the hyperbolic equation $Ae^{ky} + Be^{-ky}$. If Ω is bounded in the vertical direction by the floor placed at $y = -h(x)$ (see Fig. 5), and the reference free surface is in $y = 0$, then $g(y)$ adopts the form $\cosh[k(y+h)]$. The more general solution is given by:

$$\phi(x, y, t) = 2Ae^{-kh}\sin(kx+\alpha)\cosh(k(y+h))\,e^{i\omega t} \tag{22}$$

But ϕ needs to satisfied (20), which fixes a relation between the temporal behavior, given by $\omega(t)$, and the spatial behavior, given by $k(x)$, in the form of a *dispersion relation*:

$$\omega(k) = \sqrt{g\cdot k\cdot\tanh(kh)} \tag{23}$$

The physical amplitude η of the oscillation can be obtained from the relation $\partial\phi/\partial y = \partial\eta/\partial t$ given by Eq. (16) for $\theta \ll 1$. If we integrate $\partial\phi/\partial y$ with respect to the time, and then replace the imaginary factor $-i$ by $e^{-i(\pi/2)}$, we obtain the solution for $\eta(x, y, t)$:

$$\eta(x, y, t) = 2A\frac{k}{\omega}e^{-kh-i(\pi/2)}\sinh(k(y+h))\,e^{i(kx-\omega t)} \tag{24}$$

In the case of travelling waves, e.g., $\phi(x, y, t) = \phi_0(y)\,e^{i(kx-\omega t)}$, by a similar procedure, we obtain the solution:

$$\eta(x, y, t) = 2A\frac{k}{\omega}e^{-kh}\sinh(k(y+h))\cos(kx-\omega t) \tag{25}$$

Fig. 6 shows some isobaric lines resulting from a calculation of the temporal evolution of the waves imposed over the free surface. The superficial waves are propagated inside the domain and their amplitude decreases. It is interesting to note the jumps observed where the depth changes abruptly, as in the neighborhood of the vortex finder region.

In certain conditions, the amplitude of the wave can grow in regions where the depth is decreasing, as is seen in the case

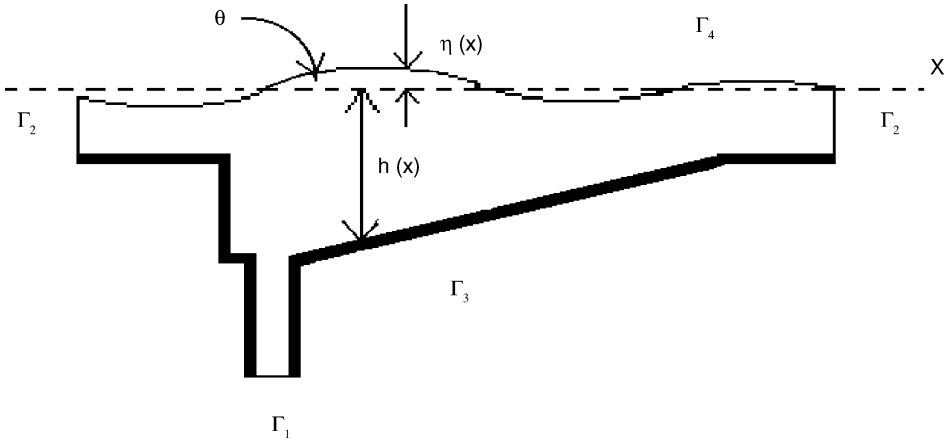

Fig. 5. Free surface.

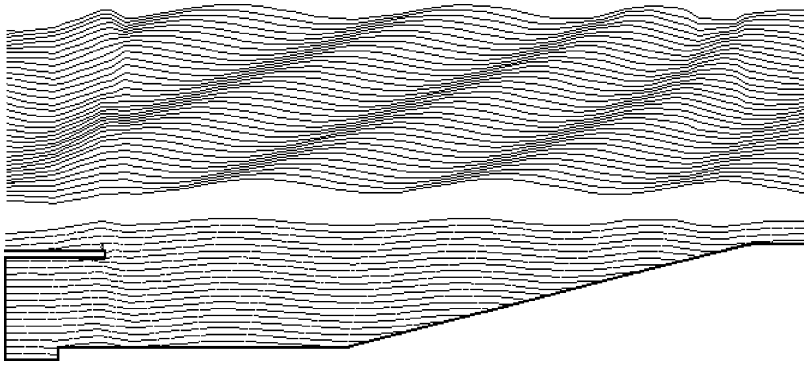

Fig. 6. Isobaric lines in the hydraulic model. In the upper figure, a temporal evolution (in vertical axis) of the free surface is shown.

of tsunamis or in the hydrocyclone apex. We suggest that in a real hydrocyclone, the intermittent suppression of flow at the apex can be due in part to the propagation and amplification of waves through the air-core.

4. Some measurements on the hydraulic model

We were interested in validating the representation of hydrocyclone physics by a simple two-dimensional hydraulic model. Toward this end, we constructed a physical model in the laboratory using translucent perspex. The experimental setup is shown in Fig. 7. The size of the model was 90 cm × 11 cm × 2 cm. Water was fed through a pipe connected at the bottom of the vortex zone. At both outlets (left: overflow, and right: underflow), the flow rate was measured. Making measurements of the water heights and calculating the mean velocity at the outlet regions, it was possible to estimate the total pressure drop in the equipment. If a pressure–flow curve is constructed, it obeys a relationship in the form $Q \sim P^{1/2}$, similar to the behavior of a real hydrocyclone. Furthermore, when the equipment is fed with different feed rates, different forms of free surface were obtained, but all showed characteristics similar to those observed in the numerical simulation of a real hydrocyclone. The flow showed a prominence at the central region and a depletion of the free surface at the outlet regions. With these arguments, we conclude that the hydraulic model can represent the principal physical features of a real hydrocyclone.

A problem that is difficult to visualize in a real hydrocyclone is the influence of the wave motion when the regime changes from spray to roping at the underflow zone of an conical hydrocyclone. There is experimental evidence [2] that the flow regimes at the apex region depend on the ratio of apex and vortex diameters D_u/D_o. When $D_u/D_o < 0.35$, the regime is always roping, and if $D_u/D_o > 0.5$, the regime is always spray. At intermediate values between 0.35 and 0.5, the behavior cannot be predicted by diameter ratio alone.

Using the hydraulic model as a physical analogy, we constructed a functional dependence between the ratios Q_u/Q_o and D_u/D_o, using the virtual radii D_o and D_u shown in Fig. 7 (distance between the free surface level and a reference and arbitrary label equivalent to the symmetry axis in a real hydrocyclone). The result is shown in Table 1. We observe that the underflow is suppressed for D_u/D_o between 0.42 and 0.3. If we induce a wave-like motion in the hydraulic model, for example, with the feed flow in a pulsating form, we obtain the response indicated by the symbol (*) in Table 1, suppressing the underflow at an earlier D_u/D_o.

To confirm our conclusions, we obtained a numerical solution for the hydrocyclone working only with water, using the commercial package FLUENT with a structured grid. The

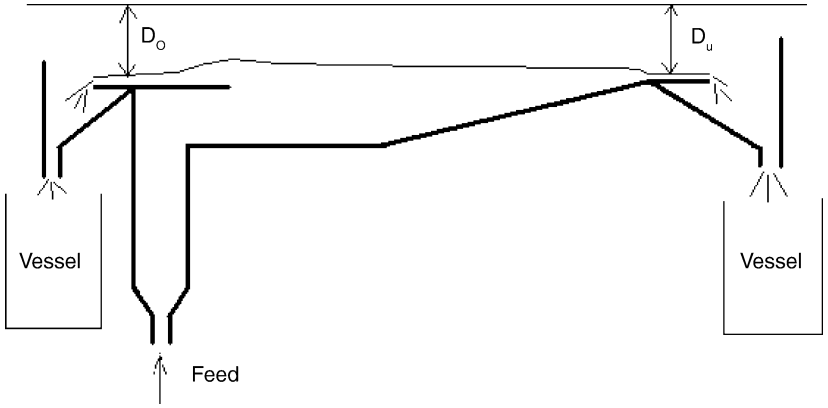

Fig. 7. Experimental setup of the hydraulic model.

Table 1
Experimental $Q_u/Q_o = f(D_u/D_o)$ relation

D_u/D_o	Q_u/Q_o	Q_u^*/Q_o^*
0.1750	0.000	0.000
0.2750	0.044	0.000
0.5750	0.349	0.183
0.7625	0.850	0.589
1.0000	2.404	2.404

Table 2
Numerical $Q_u/Q_o = f(D_u/D_o)$ relation

D_u/D_o	Q_u/Q_o	Q_u^*/Q_o^*
0.3077	0.000	0.000
0.4211	0.122	0.111
0.6154	0.289	0.289

meshes are shown in Fig. 8. For a given geometry, we do not know a priori the form of the free surface and the split ratio. The form and position of free surface are found (as was discussed before) and, for each case, we calculated a set of different values of split ratio. Finally, we chose the configuration that produced the minimum amount of mechanical energy.

To be strict, we need to compare the static solution obtained with a fixed free surface, with a time-dependent solution that considers the fluctuation of the free surface in time. In our case, however, we compared two static cases, one with and without free surface deformation. In both cases, we obtained the same result as is shown in Table 2. The behavior is similar to the measurements on the hydraulic model. For small ratios of D_u/D_o, there is a limit when the underflow disappears. In the intermediate case, given a ratio D_u/D_o, the underflow is less when there are wave-like movements at the free surface. This means that when there are oscillations, the transition between spray and roping occurs at lesser values of D_u/D_o. In other words, oscillations in discharge cause an increase in the probability of the transition from spray to roping.

5. A proposal for the origin of the waves

In this section, we explore a possible mechanism for the generation of wave-like motions in the region adjacent to the air-core in a conical hydrocyclone. The predominant force in a swirling flow is the centrifugal force. This assumes the role of a restoration force when a disturbance alters the streamlines and (as in the case of a perturbation over a tank) can, in some circumstances, manifest itself through wave-like motion. Since this kind of force appears with a change of reference frame, it is an inertial force.

In a conical hydrocyclone, the tangential velocity has the form of a forced vortex in the inner region and a free vortex in the outer region. At the inner region, the rotation is similar

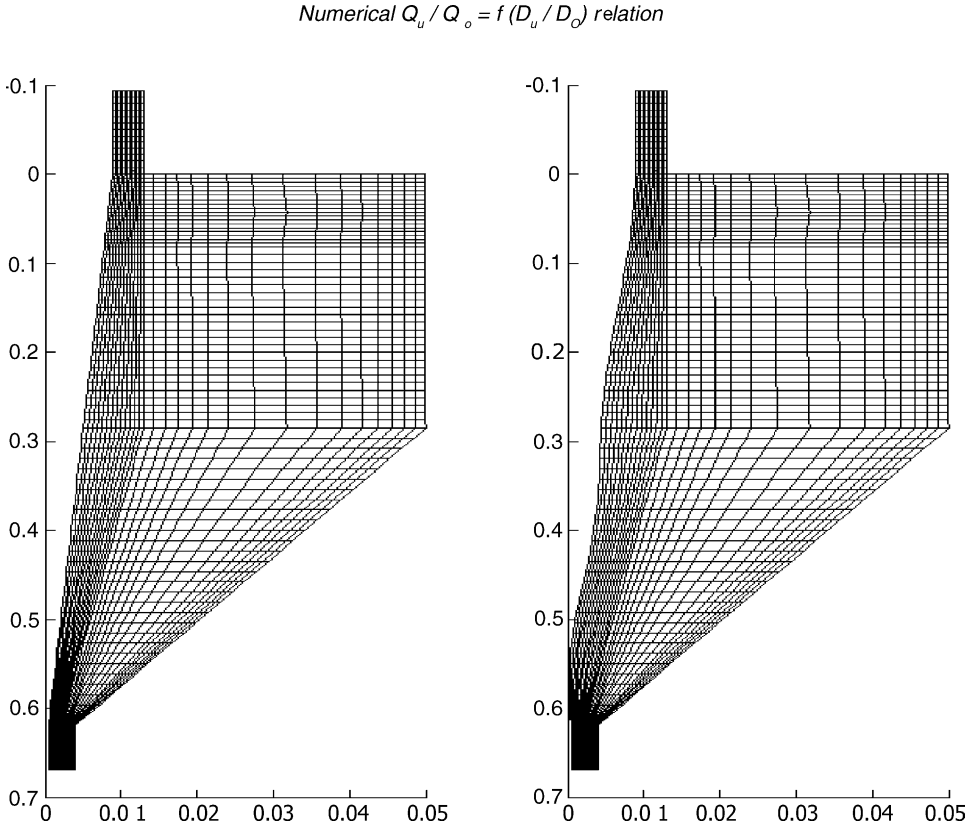

Fig. 8. Meshes used in FLUENT on a hydrocyclone.

to that of a rigid body (Taylor–Proudman theorem), and the fluid acquires some elastic properties that can sustain waves.

Our attention will be focused on the annular section surrounding the air-core, as is shown in Fig. 9. Assume that the fluid is rotating with a constant angular velocity $\mathbf{\Omega}$ around the z-axis. If the equations of motion are expressed in a reference frame rotating with the fluid, we have the two following equations:

$$\nabla \cdot \mathbf{v} = 0 \tag{26}$$

and

$$\frac{\partial \mathbf{v}}{\partial t} + \frac{1}{2}\nabla v^2 + (\nabla \times \mathbf{v}) \times \mathbf{v} + 2\mathbf{\Omega} \times \mathbf{v} + \mathbf{\Omega} \times (\mathbf{\Omega} \times \mathbf{r}) = -\frac{1}{\rho}\nabla P - \nu \nabla \times (\nabla \times \mathbf{v}) + \mathbf{F} \tag{27}$$

where $\rho(\nabla \times \mathbf{v}) \times \mathbf{v}$ is the centrifugal force, $2\rho\mathbf{\Omega} \times \mathbf{v}$ is the Coriolis force and $\mathbf{F}$ is the external force. If $\mathbf{F}$ is conservative, it can be written in terms of an arbitrary potential function Λ, and in the case of a gravitational force, we have $\mathbf{F} = -\nabla(gz)$. Grouping all gradients in one term and defining the new *pressure p* in the form:

$$p = P + \rho g z - \frac{1}{2}\rho(\mathbf{\Omega} \times \mathbf{r}) \cdot (\mathbf{\Omega} \times \mathbf{r}) \tag{28}$$

Eq. (27) adopts the form:

$$\frac{\partial \mathbf{v}}{\partial t} + (\mathbf{v} \cdot \nabla)\mathbf{v} + 2\mathbf{\Omega} \times \mathbf{v} = -\frac{1}{\rho}\nabla p - \nu \nabla \times (\nabla \times \mathbf{v}) \tag{29}$$

If L, Ω and U are characteristics dimensions of longitude, angular velocity and velocity, the importance of the centrifugal and Coriolis forces in a hydrocyclone can be estimated if the momentum equation is written in terms of the dimensionless variables $\mathbf{r}^* = \frac{r}{L}$, $t^* = t\Omega$, $\mathbf{v}^* = \frac{\mathbf{v}}{U}$, $p^* = \frac{p}{\rho\Omega UL}$ and $\nabla^* = L\nabla$. The continuity equation does not change in form, but the momentum equation changes to:

$$\frac{\partial \mathbf{v}^*}{\partial t^*} + R_0(\mathbf{v}^* \cdot \nabla^*)\mathbf{v}^* + 2\hat{\mathbf{k}} \times \mathbf{v}^* = -\nabla^* p^* - E_k \nabla^* \times (\nabla^* \times \mathbf{v}^*) \tag{30}$$

where R_0 is the Rossby number and E_k is the Ekman number defined by:

$$R_0 = \left|\frac{\rho(\mathbf{v} \cdot \nabla)\mathbf{v}}{2\rho\mathbf{\Omega} \times \mathbf{v}}\right| = \frac{\rho U L^{-1} U}{\rho\Omega U} = \frac{U}{\Omega L} \tag{31}$$

$$E_k = \left|\frac{\mu\nabla^2\mathbf{v}}{2\rho\mathbf{\Omega} \times \mathbf{v}}\right| = \frac{\mu L^{-2} U}{\rho\Omega U} = \frac{\nu}{\Omega L^2} \tag{32}$$

These numbers quantify the relative importance of the convective and viscous terms with respect to the Coriolis force. If we assume zero viscosity, the Ekman number is zero. Furthermore, if the velocity U of a perturbation is much smaller than the rotational velocity of the fluid, the Rossby number is also small. These cases are applicable to the hydrocyclone of course. In the limit case where $R_0 = 0$, the pressure force is balanced by the Coriolis force. The flow is termed geostrophic (in the future, we will drop the * in the dimensionless variables):

$$2\hat{\mathbf{k}} \times \mathbf{v} = -\nabla p \tag{33}$$

In this case, the movement is induced by a pressure field perpendicular to the path of the fluid particles, which is similar to that observed in atmospheric tornados. Applying the curl to (33) results in:

$$\hat{\mathbf{k}} \cdot \nabla \mathbf{v} = 0 \tag{34}$$

where we used the vectorial identity $\nabla \times (\hat{\mathbf{k}} \times \mathbf{v}) = \hat{\mathbf{k}}\nabla \cdot \mathbf{v} - \hat{\mathbf{k}} \cdot \nabla\mathbf{v}$. This result shows that the gradient of the velocity field does not change in the direction of the rotation axis, and the flow becomes rigid in the $\hat{\mathbf{k}}$ direction of the rotation (Taylor–Proudman theorem). In particular, if a perturbation is induced in some place, it will propagate axially through the rigid column surrounding the air-core. In the nonstationary case with $E_k = R_0 = 0$, the linear equation:

$$\frac{\partial \mathbf{v}}{\partial t} + 2\hat{\mathbf{k}} \times \mathbf{v} = -\nabla p \tag{35}$$

has a solution of the form:

$$\mathbf{v}(\mathbf{x}, t) = \mathbf{V}(\mathbf{x})\, e^{i\omega t} \tag{36}$$

$$p(\mathbf{x}, t) = P(\mathbf{x})\, e^{i\omega t} \tag{37}$$

where ω is the angular frequency of a perturbation imposed on the flow. The equations of motion are now:

$$\nabla \cdot \mathbf{V} = 0 \tag{38}$$

$$i\omega\mathbf{V} + 2\hat{\mathbf{k}} \times \mathbf{V} = -\nabla P \tag{39}$$

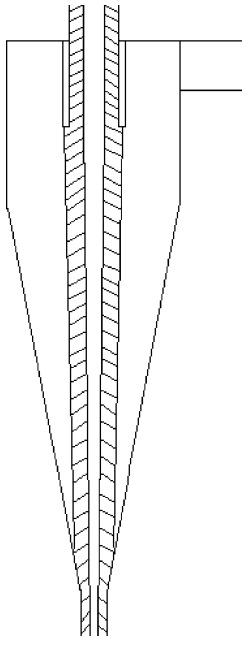

Fig. 9. Zone for generation of inertial waves in the hydrocyclon.

The last equation couples the velocity and pressure fields. It is convenient to express both equations in terms of only the pressure variable. Applying the curl to Eq. (39), and using the vectorial identity $\nabla \times (\mathbf{A} \times \mathbf{B}) = \mathbf{B} \cdot \nabla \mathbf{A} - \mathbf{A} \cdot \nabla \mathbf{B} + \mathbf{A} \nabla \cdot \mathbf{B} - \mathbf{B} \nabla \cdot \mathbf{A}$, we obtain:

$$\nabla \times \mathbf{V} = -\frac{2i}{\omega} \hat{\mathbf{k}} \cdot \nabla \mathbf{V} \tag{40}$$

If we apply the k component of the gradient $(\hat{\mathbf{k}} \cdot \nabla)$ to (39) equation, we have:

$$\hat{\mathbf{k}} \cdot \nabla \mathbf{V} = \frac{i}{\omega} \hat{\mathbf{k}} \cdot \nabla \nabla P \tag{41}$$

Combining Eqs. (40) and (41) and taking the divergence of (39), we obtain the Poincare equation:

$$\nabla^2 P - \frac{4}{\omega^2} (\hat{\mathbf{k}} \cdot \nabla)^2 P = 0 \tag{42}$$

Now, it is necessary to convert the boundary condition $\mathbf{V} \cdot \mathbf{n} = 0$ into an equation in terms of P. Projecting (39) on the vector $\mathbf{n} \times \hat{\mathbf{k}}$, and using the vectorial identity $(\mathbf{a} \times \mathbf{b}) \cdot (\mathbf{c} \times \mathbf{d}) = (\mathbf{a} \cdot \mathbf{c})(\mathbf{b} \cdot \mathbf{d}) - (\mathbf{a} \cdot \mathbf{d})(\mathbf{b} \cdot \mathbf{c})$, we have:

$$(i\omega(\hat{\mathbf{k}} \times \mathbf{V}) - 2\mathbf{V}) \cdot \mathbf{n} + \frac{2i}{\omega} \mathbf{n} \cdot \hat{\mathbf{k}} \hat{\mathbf{k}} \cdot \nabla P = -(\mathbf{n} \times \hat{\mathbf{k}}) \cdot \nabla P \tag{43}$$

and replacing $\hat{\mathbf{k}} \times \mathbf{V}$ from (39) in (43), we obtain:

$$i\omega^2 \left(\omega - \frac{4}{\omega} \right) \mathbf{V} \cdot \mathbf{n} = \omega^2 \mathbf{n} \cdot \nabla P - 4(\mathbf{n} \cdot \hat{\mathbf{k}})(\hat{\mathbf{k}} \cdot \nabla P) - 2i\omega(\hat{\mathbf{k}} \cdot \mathbf{n}) \cdot \nabla P \tag{44}$$

Then, the boundary condition $\mathbf{V} \cdot \mathbf{n} = 0$ expressed in terms of P is given by (44) with the first term equal to zero. This equation is hyperbolic for $|\omega| \leq 2$ and elliptic in the other case. In the first case, the solution is in the form of waves.

5.1. The numerical solution

The solution to Eq. (42) can be obtained in a FEM context. In the derivation that follows, we use the term ϕ in place of P, and ϕ^* will be the conjugate of ϕ. We choose $\phi \propto \exp(ik\theta)$. Applying the Galerkin method, we multiply (42) by ϕ^* and then integrate:

$$\int_\Omega \phi^* (\omega^2 \nabla^2 \phi - 4 \nabla \cdot \hat{k}\hat{k} \cdot \nabla \phi) \, \mathrm{d}V = 0 \tag{45}$$

For the first term, we use the vectorial identity $\nabla \cdot (\phi^* \nabla \phi) = \phi^* \nabla^2 \phi + \nabla \phi^* \cdot \nabla \phi$ and $\nabla \cdot (\phi^* \hat{k}\hat{k} \cdot \nabla \phi) = \phi^* \nabla \cdot \hat{k}\hat{k} \cdot \nabla \phi + \nabla \phi^* \cdot \hat{k}\hat{k} \cdot \nabla \phi$ for the second. Then:

$$\int_\Omega (\omega^2 (\nabla \phi^* \cdot \nabla \phi) - 4 \nabla \phi^* \cdot \hat{k}\hat{k} \cdot \nabla \phi) \, \mathrm{d}V + \int_{\partial\Omega} (-\omega^2 \phi^* \nabla \phi + 4 \phi^* \hat{k}\hat{k} \cdot \nabla \phi) \cdot \hat{n} \, \mathrm{d}S = 0 \tag{46}$$

Using Eq. (44) as a boundary condition, the term in the surface integral can be transformed to:

$$2\omega i \int_{\partial\Omega} \phi^* (\hat{k} \times \nabla \phi) \cdot \hat{n} \, \mathrm{d}S \tag{47}$$

The next step is to rewrite (46) in cylindrical coordinates. Then $\phi = \psi \, \mathrm{e}^{ik\theta}$ and the gradient of ϕ becomes:

$$\nabla \phi = \left(\frac{\partial \psi}{\partial r} \hat{r} + \frac{ik}{r} \psi \hat{\theta} + \frac{\partial \psi}{\partial z} \hat{k} \right) \mathrm{e}^{ik\theta} \tag{48}$$

The volume element is $\mathrm{d}V = r \, \mathrm{d}r \, \mathrm{d}\theta \, \mathrm{d}z$. Eq. (48) can now be written as:

$$\int_{\partial\Omega} \left[\omega^2 r \left(\frac{\partial \psi}{\partial r} \right)^2 - (4 - \omega^2) r \left(\frac{\partial \psi}{\partial z} \right)^2 + \frac{k^2 \omega^2}{r} \psi^2 \right] \mathrm{d}\Sigma + 2k\omega \int_{\partial\partial\Omega} (\hat{r} \cdot \hat{n}) \psi^2 \, \mathrm{d}l = 0 \tag{49}$$

where $\mathrm{d}\Sigma = 2\pi r \, \mathrm{d}r \, \mathrm{d}z$ and $\mathrm{d}l$ are the differentials of surface and line elements, respectively. Writing ψ in terms of a linear combination of nodal values ψ_i, as $\psi = \sum_{i=1}^{N_p} N_i \psi_i$, the last equation has the form of a nonlinear matrix equation in ω:

$$(\omega^2 [A] + \omega [B] + [C]) \{\psi\} = 0 \tag{50}$$

with A_{ij}, B_{ij} and C_{ij} given by:

$$A_{ij} = \int_\Omega \left(r \frac{\partial N_i}{\partial r} \frac{\partial N_j}{\partial r} + r \frac{\partial N_i}{\partial z} \frac{\partial N_j}{\partial z} + \frac{k^2}{r} N_i N_j \right) \mathrm{d}\Sigma \tag{51}$$

$$B_{ij} = 2k \int_{\partial\Omega} \hat{\mathbf{r}} \cdot \hat{\mathbf{n}} N_i N_j \, \mathrm{d}l \tag{52}$$

$$C_{ij} = -4 \int_\Omega r \frac{\partial N_i}{\partial z} \frac{\partial N_j}{\partial z} \, \mathrm{d}\Sigma \tag{53}$$

The explicit forms of the matrices are:

$$A_{ij} = r_c^2 K_{ij} + \frac{k^2 r_c \Delta}{6} \begin{bmatrix} 2 & 1 & 1 \\ 1 & 2 & 1 \\ 1 & 1 & 2 \end{bmatrix} \tag{54}$$

$$B_{ij} = 2k\hat{\mathbf{r}} \cdot \hat{\mathbf{n}} \frac{|P_2 - P_1|}{6} \begin{bmatrix} 2 & 1 \\ 1 & 2 \end{bmatrix} \tag{55}$$

$$C_{ij} = -\frac{2r_c^2}{A} \begin{bmatrix} (r_3 - r_2)^2 & (r_3 - r_2)(r_1 - r_3) & (r_3 - r_2)(r_2 - r_1) \\ (r_3 - r_2)(r_1 - r_3) & (r_1 - r_3)^2 & (r_1 - r_3)(r_2 - r_1) \\ (r_3 - r_2)(r_2 - r_1) & (r_1 - r_3)(r_2 - r_1) & (r_2 - r_1)^2 \end{bmatrix} \tag{56}$$

$$K_{ij} = \frac{1}{2\Delta} \begin{bmatrix} z_{23}^2 + r_{23}^2 & z_{13}z_{32} + r_{13}r_{32} & z_{23}z_{12} + r_{23}r_{12} \\ z_{13}z_{32} + r_{13}r_{32} & z_{31}^2 + r_{31}^2 & z_{21}z_{13} + r_{21}r_{13} \\ z_{23}z_{12} + r_{23}r_{12} & z_{21}z_{13} + r_{21}r_{13} & z_{12}^2 + r_{12}^2 \end{bmatrix} \tag{57}$$

where Δ is the area of each triangle and $r_c = (r_1 + r_2 + r_3)/3$.

In our problem, some points of ψ belong to the boundary of the domain and others are interior points. In a manner similar to the computation of the modes of vibration of a membrane, we can consider that some boundaries are fixed and others free. If point i belongs to a boundary, where ψ is fixed, we will put $\psi_i = 0$. Then we can split the solution field ψ into two disjoint groups: $\psi = \psi^0 \cup \psi^f$, where ψ^0 represents the collection of points where $\psi = 0$, and ψ^f the rest. The eigenvalue Eq. (50) must be applied strictly to the ψ^f group of points.

The quadratic eigenvalue Eq. (50) can be solved as follows. Let $\{\phi\} = \omega\{\psi^f\}$; then we can rewrite (50) as the two following equations:

$$[A]\{\phi\} = \omega[A]\{\psi^f\} \tag{58}$$

and

$$\omega[A]\{\phi\} + [B]\phi + [C]\{\psi^f\} \tag{59}$$

Eqs. (58) and (59), which are linear in ω but with coupled eigenvalues ψ^f and ϕ, can be written in a form of a linear system:

$$\begin{bmatrix} 0 & [A] \\ -[C] & -[B] \end{bmatrix} \begin{Bmatrix} \psi^f \\ \phi \end{Bmatrix} = \omega \begin{bmatrix} [A] & 0 \\ 0 & [A] \end{bmatrix} \begin{Bmatrix} \psi^f \\ \phi \end{Bmatrix} \tag{60}$$

This equation can be solved with the usual methods.

We solved two cases. For simplicity, we consider only the axisymmetric modes ($k = 0$). The first case considers a cylindrical pipe of 165 cm in length and with internal and external radii of 3 mm and 13 cm, respectively. The second case is again a cylindrical pipe, but with the external radii varying from 13 cm at the top (height of 50 cm) to 6 cm at the bottom.

We use the following boundary conditions. Fix the values of the pressure at the top and bottom of the cylinders to zero, and let the boundaries at the radial walls be free. This selection is based on the fact that at the internal radius, the air-core is free to acquire any form at the interior because of the negligible air resistance. The same effect is valid for the external radius because here, the external fluid behaves as a free vortex.

Fig. 10 shows the results of both cases. In each row, the geometry of the domain is shown first and then the first four modes for the pressure field. It is interesting to compare this behavior with that observed in the dispersion of the axial velocities obtained with laser-Doppler anemometer in a conical hydrocyclone (Fig. 11b) [5]. The measurements showed a greater dispersion of the axial velocity in the center compared to the upper and lower regions. This behavior can be explained by the presence of vertical fluctuations of the axial component of velocity.

The next observation is the abrupt oscillation observed where the external radius changes in the case of the variable cylinder compared to the behavior of the cylinder of constant external radius. As had been suggested by the hydraulic model, the apex region is a zone were some instabilities can grow. This can explain, for example, the pulsating character of the exit flow, when a hydrocyclone operates in a transition regime between spray and roping.

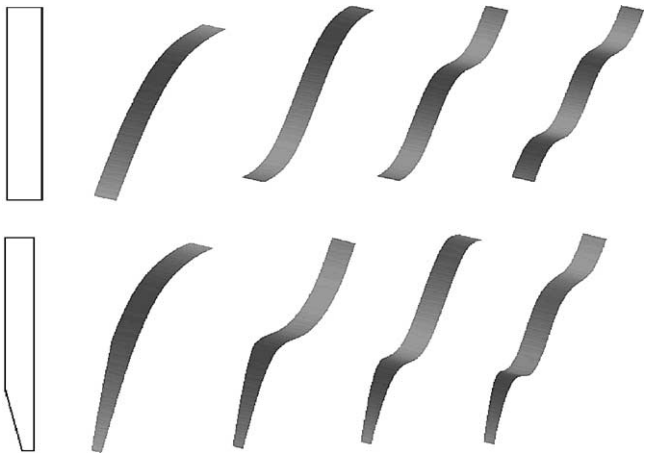

Fig. 10. Oscillation modes for a pressure field, (up) using a cylindrical and, (below) using a modified cylindrical pipe. When the radius of cylinder shrink, the pressure distributions loss symmetry.

Finally, several other modes of inertial oscillations can be induced by different types of motions. Precession and vibration have been observed at the free surface of the air-core in industrial hydrocyclones.

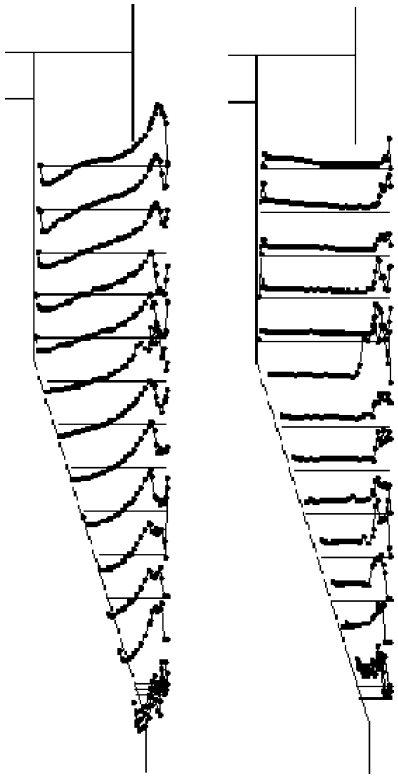

Fig. 11. (a) Mean and (b) variance of the axial velocity component in a conical hydrocyclone, obtained by LDA technique.

6. Conclusions

Using some simple arguments, we have shown some important features of the dynamics of a conical hydrocyclone.

(1) We have shown that the form of the free surface depends mainly on the global geometrical characteristics of the flow and possibly, to a minor extent, on physicochemical properties of the free surface.
(2) We have shown that the air-core plays an important role in the phenomenon of roping, as is suggested by the pulsating character that is observed in the underflow, when the regime changes from spray to roping. This phenomenon may be induced by the loss of stability in a region near the apex. Then, on average, the air-core increases in diameter with the possibility of reaching a size close to the apex diameter. In such a case, roping may be induced. This effect is enhanced by the presence of oscillations in the free surface, which increase in amplitude close to the apex.
(3) The oscillations can be forced by several physical reasons, for example, by pressure fluctuations introduced into the hydrocyclone through the feed. In this work, we suggest that a relevant physical source of oscillations is by the generation and propagation of inertial waves induced in the neighborhood of the air-core, where the tangential velocity behaves as a rigid body. The amplitude of these oscillations can in some cases be stationary, as suggested by the dispersion of the axial velocity component measured in the laboratory. In other cases, the superficial waves can travel through the free surface, as is observed in transparent models.
(4) Waves propagating through the water–air interface of the air-core will increase their amplitude as the hydrocyclone diameter becomes smaller and may become of the order of the apex, in which case an instability is induced in the underflow. The apex would intermittently become blocked by the air-core, inducing roping. The presence of waves in a conical hydrocyclone is not desirable because they promote the occurrence of roping and introduce an additional perturbation on the particles that are being classified. Unfortunately, their existence is inherent in the physics of the flow.

Acknowledgements

We acknowledge the financial support of Fondecyt under Project No. 2980005, Fondef MI-08 and F-1064, from the Graduate School and Research Council of the University of Concepción and from the Mineral Technology Center CETTEM. We also acknowledge the helpful collaboration of Professor Rodolfo Rodriguez from Mathematics Department of the University of Concepción for his comments on the solution of the quadratic eigenvalue equation.

References

[1] A. Barrientos, R. Sampaio, F. Concha, Effect of the air core on the performance of a hydrocyclone, in: XVIII International Mineral Processing Congress, Sydney, 23–28 May, 1993, pp. 267–270.
[2] M.O. Bustamante, Efecto de la geometría de un hidrociclón sobre las condiciones normales de operación, M.Sc. Thesis, Universidad de Concepción, 1991.
[3] F. Concha, A. Barrientos, J. Montero, R. Sampaio, Air core and roping in hydrocyclones, in: Eighth European Symposium on Comminution, Stockholm, 1994, pp. 814–823.
[4] O. Castro, F. Concha, J. Montero, J. Miranda, J. Castro, D. Urizer, Air core modelling for an industrial hydrocyclone, in: D. ClaxFon, L. Svarovsky, M.T. Theo (Eds.), Hydrocyclones-96, MEP Ltd., London, 1996.
[5] B. Chine, Unpublished measurements, 1996.
[6] F. Concha, A. Barrientos, J. Montero, R. Sampaio, Air core and roping in hydrocyclones, Int. J. Min. Proc. 44 (1996) 743–749.
[7] T. Dyakowski, R.A. Williams, Prediction of air core size and shape in a hydrocyclone, Int. J. Min. Proc. 43 (1995) 1–14.
[8] M.P. Escudier, J. Bornstrein, T. Maxworthy, The dynamics of confined vortices, Proc. R. Soc. Lond. A 382 (1982) 335–360.
[9] Q. Luo, C. Deng, J. Xu, L. Yu, G. Xiong, Comparison of the performance of water-sealed and commercial hydrocyclones, Int. J. Min. Proc. 25 (1989) 297–310.
[10] E. Ovalle, F. Concha, The role of wave propagation in hydrocyclone operations. I. An axi-symmetric stream-function formulation for a conical hydrocyclone, J. Chem. Eng., submitted for publication.
[11] A.R. Paterson, A First Course in Fluid Dynamics, Cambridge University Press, 1983.
[12] R.A. Williams, O. Ilyas, T. Dyakowski, Air core imaging in cyclone coal separator using electrical resistance tomography, Coal Prep. 15 (1995) 143–163.